Aerodynamic Optimization of Box-Wing Planform Through Machine Learning Integration

HASAN Mehedi[1], *DENG Zhongmin*[1*], *REDONNET Stéphane*[2*], *SANUSI B. Muhammad*[3]

1. Hangzhou International Innovation Institute, Beihang University, Hangzhou 310020, P. R. China; 2. Department of Mechanical and Aerospace Engineering, Hong Kong University of Science and Technology, Hong Kong 999077, P. R. China; 3. School of Mechanical Engineering and Automation, Harbin Institute of Technology, Shenzhen 518057, P. R. China

(Received 18 June 2025; revised 20 September 2025; accepted 5 October 2025)

Abstract: This study discusses a machine learning-driven methodology for optimizing the aerodynamic performance of both conventional, like common research model (CRM), and non-conventional, like Bionica box-wing, aircraft configurations. The approach leverages advanced parameterization techniques, such as class and shape transformation (CST) and Bezier curves, to reduce design complexity while preserving flexibility. Computational fluid dynamics (CFD) simulations are performed to generate a comprehensive dataset, which is used to train an extreme gradient boosting (XGBoost) model for predicting aerodynamic performance. The optimization process, using the non-dominated sorting genetic algorithm (NSGA-Ⅱ), results in a 12.3% reduction in drag for the CRM wing and an 18% improvement in the lift-to-drag ratio for the Bionica box-wing. These findings validate the efficacy of machine learning based method in aerodynamic optimization, demonstrating significant efficiency gains across both configurations.

Key words: aerodynamic optimization; box-wing; machine learning; computational fluid dynamics (CFD)

CLC number: TN925 **Document code**: A **Article ID**: 1005-1120(2025)06-0789-12

0 Introduction

Modern air transportation faces significant challenges, particularly the need to reduce its environmental impact. Chemical emissions are a major obstacle to sustainability, worsened by the sector's annual growth of about 5%. Optimizing aircraft design offers a solution by maximizing transport capacity and minimizing fuel consumption. This can be achieved by enhancing lifting capabilities (increasing payload) and reducing drag (lowering propulsion power in cruise), thus improving aerodynamic performance and maximizing the lift-to-drag (L/D) ratio. Research in this area ranges from conservative methods like passive flow control[1] to more innovative approaches involving novel aircraft and power plant architectures. Researchers are also exploring some non-conventional designs like blended wing body or box wing[2] planform for the potential solutions.

In recent years, significant progress has been made in aerodynamic optimization, particularly in wing design, relying on computational fluid dynamics (CFD) and adjoint-based optimization[3-12] to balance accuracy and computational efficiency. However, optimizing an aircraft wing remains challenging due to the complexity of design spaces and the high computational cost. The widespread adoption of machine learning (ML) techniques, such as deep neural networks (DNNs), has started addressing these challenges, with applications in fluid mechanics, including airfoil and wing optimization[13-17]. Using ad-

*Corresponding authors, E-mail addresses: dengzhongmin@buaa.edu.cn; redonnet@ust.hk.

How to cite this article: HASAN Mehedi, DENG Zhongmin, REDONNET Stéphane, et al. Aerodynamic optimization of box-wing planform through machine learning integration[J]. Transactions of Nanjing University of Aeronautics and Astronautics, 2025,42(6):789-800.

http://dx.doi.org/10.16356/j.1005-1120.2025.06.006

vanced parameterization techniques like class and shape transformation (CST) reduces design variables and dataset sizes, improving optimization efficiency. Various ML algorithms, including random forest (RF), stochastic gradient tree boosting (SGTB), and extreme gradient boosting (XGBoost)[9,18-19], have shown promise in aerodynamic optimization with smaller datasets. To the authors' best knowledge, however, the aerodynamic optimizations of representative transonic wings or box-wings using these advanced ML-based strategies (e.g., CST, XGBoost) are yet to be assessed.

This paper summarizes the ML based aerodynamic optimization approach, which is validated by using the well-known common research model (CRM) benchmark proposed by National Aeronautics and Space Administration (NASA). Then, the application of these ML-based techniques is extended to the aerodynamic optimization of a conceptual box wing planform.

1 Methodology

This study focuses on optimizing the box-wing configuration through a low-fidelity ML approach. This methodology leads us to a solution space aligned with our objectives, following the ISO 9001:2015 process approach for structured development[20-21]. In line with this framework, the methodology includes three components: Input, process, and output[20]. The input phase provides the necessary requirements and resources, while the process phase follows the plan-do-check-act (PDCA) cycle to drive operations[21-22]. Finally, the output phase aims to meet the objectives defined by the input phase.

To implement the ISO 9001:2015 process approach, we first identify and organize the elements of input, process, and output. Key steps include parameterization, random sampling, numerical solving, and data preparation, which yield the initial output, the training dataset. This dataset then undergoes further processing, including ML algorithm training, initial model prediction, test set allocation, and average prediction error (APE) calculations. Based on tolerance limits, the final output is a surrogate model. This surrogate model interfaces with the subsequent "optimizer" process, which considers objectives and constraints as inputs, ultimately producing the final output: The "optimized parameters" that represent the optimised geometry. This iterative process adheres to the PDCA cycle, ensuring that the initial inputs and outputs contribute and influence the generation of the final output. This demonstrates the inter-connected and continuous refinement of the methodology. All these processes are illustrated in the Fig.1.

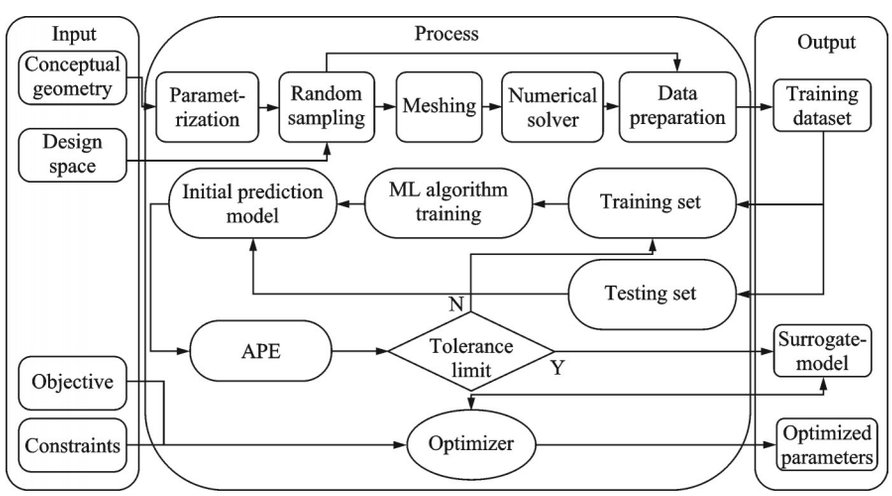

Fig.1 Demonstration of the proposed optimization framework

The process involves parameterization, computation, sampling, surrogate model development, validation, and optimization. For the first step, the baseline airfoil for both configuration are parameterized using CST approach. Here, the inverse approach is taken, which first initializes random CST

coefficients, then performs optimization to reduce the error between the baseline and CST defined airfoil. Once the CST defined airfoil reaches the error less than 1%—2% from the baseline, the CST coefficients are finalized for the airfoil. Now, the baseline wing planform are discretized along the span. Here, the number of section and the location of the section along the span is determined based on the shape of the baseline model. For example, seven equally spaced sections on CRM wing has found efficient to capture the baseline shape, while the box wings required more sections as it shape changes, e.g. dihedral, chord etc., frequently along the span. The sectional parameter distribution along the span is parameterized with Bezier curves (B-curves) to minimize total variables count. Multiple samples are generated within the design space and solved by CFD solvers to create a dataset for machine learning. A surrogate model is then constructed, followed by optimization using the non-dominated sorting genetic algorithm (NSGA-Ⅱ) to refine geometry. This entire process (Fig.2) is automated through in-house code that integrates all steps.

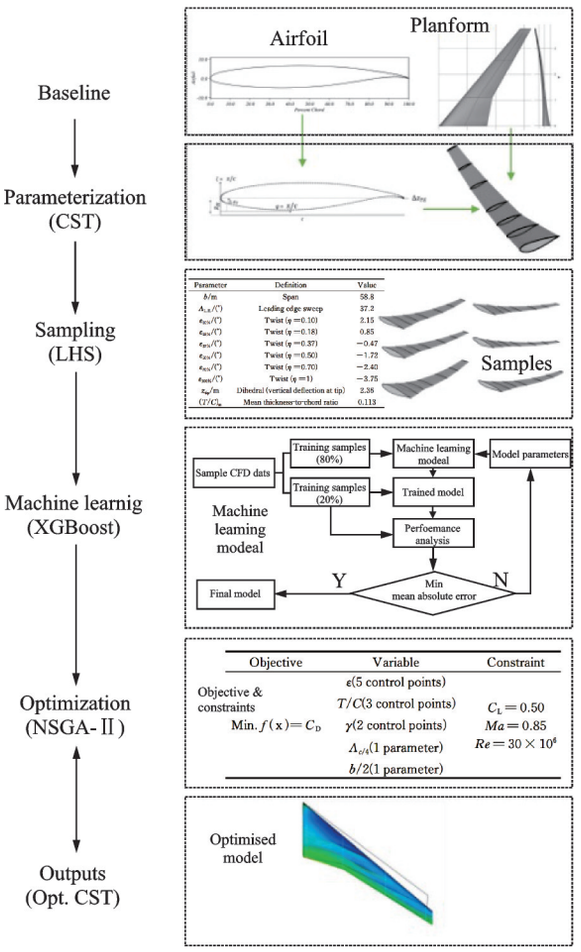

Fig.2 Flowchart of the proposed optimization approach

2 Applications

2.1 Parameterization of the planforms

To ease its subsequent deformation within an automated script, the baseline geometries are first parameterized, this being achieved using the so-called CST method. CST provides enhanced control over the wing shape, avoiding the aerodynamically inefficient or mesh-incompatible geometries noted in previous studies[23-24].

Fig.3 illustrates the CST-generated airfoil for the CRM wing at 65% of its half-span ($\eta = 0.65$) and the Clark Y airfoil used in the Bionica box wing configuration. The parametric airfoils comprise approximately 200 points and are generated using only a dozen binomial weight parameters, as shown in Fig.3, where c denotes the normalized chord, x and z denote the horizontal and the vertical coordinates, respectively, and α_t denotes the twist angle.

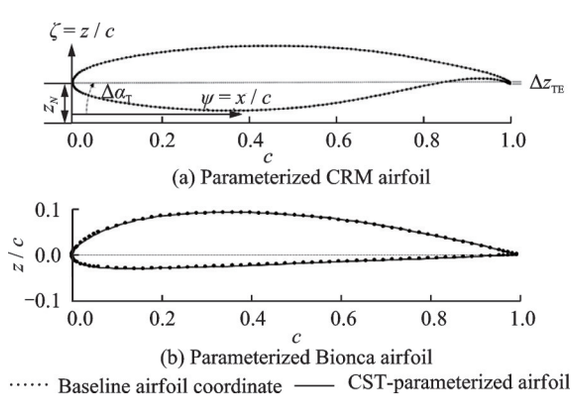

Fig.3 CST-generated airfoils of the wing profiles for both the CRM and Bionica baseline airfoils

The wing planforms are parameterized by replicating airfoil sections at specified spanwise locations. For the CRM wing, representing a conventional tube-wing configuration, this spanwise positioning with planform parameters is sufficient to reconstruct the geometry. In contrast, the box wing requires a more detailed approach: It consists of a front wing similar to the CRM wing, a rear wing that is forward-swept and structurally distinct, and vertical winglets connected through blended junc-

tions. As a result, the box-wing geometry demands a larger number of sections and careful placement to accurately capture its features.

For the CRM wing, seven sections were defined, with their locations (as percentages of the semi-span) obtained from the reference study[10]. In the case of the box wing, six sections were identified as sufficient, based on iterative comparisons between the parameterized model and the original CAD geometry. For both the CRM and box-wing models, the best practice is to align the parametric sections with the baseline CAD geometry to ensure accuracy. To maintain continuous control of the section parameters, Bezier curve fitting with a minimal number of control points is employed. This approach is particularly important for accurately capturing the smooth transitions at the blended junctions of the box wing. For the box wing's blended junction, a parametric equation incorporating three functions has been established.

$$X_r = X(s) - R\sin\theta\tan s_\varphi \tag{1}$$

$$Y_r = Z(s)\sin\theta - R\sin\theta \tag{2}$$

$$Z_r = (Z(s)\cos\theta - R\cos\theta) + \tan t_\varphi \tag{3}$$

where X_r is responsible for describing the airfoil's rotation around the central axis. This rotation is key to determining the airfoil's orientation at various sections along the span (junction) of the wing. θ, s_φ, t_φ stand for the orientation (degrees) of the local airfoil section along Y, Z, X axises; $X(s)$ and $Z(s)$ are the airfoils coordinates; R defines the diameters of the bending at the junction which can be adjusted based on the vertical distance between the front and the rear wings; Y_r and Z_r functions specify the leading-edge point's position of winglet, used to define the sweep and the twist, for each individual airfoil section.

The resulting CRM wing has a semi-span of 26.44 m and a wetted area of 167.20 m^2, matching the counterpart[10] (Fig.4). Its Bezier curve-based parameterization allows easy modifications by adjusting control points. The wing shape and deformation require only 147 parameters, significantly fewer than traditional methods like free form deformation (FFD)[10]. Plus, Bionica has 7.5 m semi-span

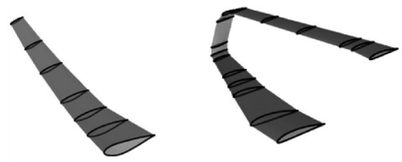

(a) Baseline CRM (b) Bionica

Fig.4 CST-generated airfoils wing planforms for both configurations

for both wings and result in total wetted area of 16 m^2, matching our previous study[25-26]. The parameters used to define the CRM and Bionica wing planforms are consistent with the previous low-fidelity study. Tables 1,2 present these parameters along with their baseline values.

Table 1 CRM wing baseline parameters[25]

Parameter	Definition	Value
b/m	Span	58.8
$\Lambda_{L.E.}$/(°)	Leading edge sweep	37.2
$\varepsilon_{10\%}$/(°)	Twist (η =0.10)	2.15
$\varepsilon_{18\%}$/(°)	Twist (η =0.18)	0.85
$\varepsilon_{37\%}$/(°)	Twist (η =0.37)	−0.47
$\varepsilon_{50\%}$/(°)	Twist (η =0.50)	−1.72
$\varepsilon_{70\%}$/(°)	Twist (η =0.70)	−2.40
$\varepsilon_{100\%}$/(°)	Twist (η =1)	−3.75
z_{tip}/m	Dihedral (vertical deflection at tip)	2.36
$(T/C)_m$	Mean thickness-to-chord ratio	0.113

2.2 Dataset generation

Creating a diverse dataset is essential for building a comprehensive training repository for ML optimization. The number of samples in the dataset scales with the parameters is considered. Thus, only the key geometric parameters known to significantly influence the overall L/D performance of the wing are chosen. These include wingspan, leading-edge sweep, twist angles at specified spanwise stations, dihedral angle, and the wingtip thickness-to-chord ratio (Tables 1, 2). Each metric is explored within a design space centered on the baseline values, with most varied within 15%—20% of the baseline, and extrema chosen to allow sufficient exploration while remaining reasonable (Tables 3, 4). Metrics are discretized into 15—20 samples per variable (SPV)[27-28], providing optimal granularity without overfitting[29], and keeping data points manageable for computation[30]. The sample

Table 2 Bionica wing baseline parameters[25]

Wing	Parameter	Definition	Value
Front wing	$\Lambda_{0.2(c/4)}$/(°)	Sweep (25% chord) at 20% of $b/2$	23.46
	$\Lambda_{1.0(c/4)}$/(°)	Sweep (25% chord) at tip	18.46
	$b/2$/m	Semi span	6.5
	$\varepsilon_{0.0}$/(°)	Twist (root)	0.0
	$\varepsilon_{0.4}$/(°)	Twist (40% of $b/2$, kink)	0.0
	$\varepsilon_{1.0}$/(°)	Twist (root)	0.0
	$\gamma_{0.0}$/(°)	Dihedral (root)	0.00
	$\gamma_{0.4}$/(°)	Dihedral (40% of $b/2$, kink)	15.00
	$\gamma_{1.0}$/(°)	Dihedral (tip)	17.00
	$T/C_{0.0}$	Thickness to chord ratio (root)	0.11
	$T/C_{0.4}$	Thickness to chord ratio (40% of $b/2$, kink)	0.11
	$T/C_{1.0}$	Thickness to chord ratio (tip)	0.11
	C_r/m	Chord (root)	2.7
	MAC/m	Mean aerodynamic chord	1.66
	C_t/m	Chord (tip)	0.98
Rear wing	$\Lambda_{c/4}$/(°)	Sweep (25% chord) at tip	−20.56
	$b/2$/m	Semi span	6.5
	$\varepsilon_{0.0}$/(°)	Twist (root)	0.0
	$\varepsilon_{0.4}$/(°)	Twist (40% of $b/2$)	0.0
	$\varepsilon_{1.0}$/(°)	Twist (root)	0.0
	$\gamma_{0.0}$/(°)	Dihedral (root)	0.00
	$\gamma_{0.4}$/(°)	Dihedral (40% of $b/2$, kink)	0.00
	$\gamma_{1.0}$/(°)	Dihedral (tip)	0.00
	$T/C_{0.0}$	Thickness to chord ratio (root)	0.11
	$T/C_{0.4}$	Thickness to chord ratio (40% of $b/2$, kink)	0.11
	$T/C_{1.0}$	Thickness to chord ratio (tip)	0.11
	C_r/m	Chord (root)	1.26
	C_t/m	Chord (tip)	0.86
Winglet	H/m	Height	1.2
	Λ_h/(°)	Sweep	30

Table 3 Design space for the CRM wing

Parameter	Lower bound	Upper bound
b/m	56	64
$\Lambda_{L.E.}$/(°)	30	44
$\varepsilon_{10\%}$/(°)	1	6
$\varepsilon_{18\%}$/(°)	−1	4
$\varepsilon_{37\%}$/(°)	−1	4
$\varepsilon_{50\%}$/(°)	−2	2
$\varepsilon_{70\%}$/(°)	−3	2
$\varepsilon_{100\%}$/(°)	−4	−1
z_{tip}/m	1.40	2.40
$(T/C)_m$	0.08	0.120

Table 4 Design space for the Bionica configurations[25]

Wing	Parameter	Lower bound	Upper bound
Front wing	$\Lambda_{0.2(c/4)}$/(°)	10	25
	$\Lambda_{1.0(c/4)}$/(°)	20	30
	$\varepsilon_{0.0}$/(°)	0.0	8.0
	$\varepsilon_{0.4}$/(°)	4.0	6.0
	$\varepsilon_{1.0}$/(°)	−3.0	3.0
	$\gamma_{0.4}$/(°)	10.0	25.0
	$\gamma_{1.0}$/(°)	17.0	26.0
	$T/C_{0.0}$	0.08	0.11
	$T/C_{0.4}$	0.05	0.08
	$T/C_{1.0}$	0.03	0.05
Rear wing	$\Lambda_{1.0(c/4)}$/(°)	−15	−30
	$\varepsilon_{0.0}$/(°)	0.0	6.0
	$\varepsilon_{1.0}$/(°)	−3.0	3.0
	$\gamma_{1.0}$/(°)	−3.00	0.00
	$T/C_{0.0}$	0.08	0.11
	$T/C_{1.0}$	0.03	0.05
Winglet	Λ_w/(°)	25	35

generation process began with 15 samples per variable, and the number of samples is progressively increased until the ML model exhibits a prediction error of less than 10% compared to the CFD results. This procedure yields 160 CRM-based and 400 Bionica-based planform samples, which are used to train an XGBoost model. The resulting ML model achieves an average prediction error of approximately 6% relative to the CFD data. Beyond this point, further increasing the sample size does not yield any noticeable improvement in predictive performance.

2.3 Meshing and computation

Each planform is automatically characterized aerodynamically using CFD, following guidelines from our previous study[31]. Due to symmetry, only half of the geometry is modeled, with the symmetry plane at the wing root. The computational domain extends approximately 50×28×28 mean aerodynamic chords in axial, lateral, and vertical directions, and is meshed with an unstructured grid (Fig.5) using commercial software integrated into the optimization platform.

The ultimate mesh contains around 1.7 million hexa-hedral elements, 98% of which maintain good

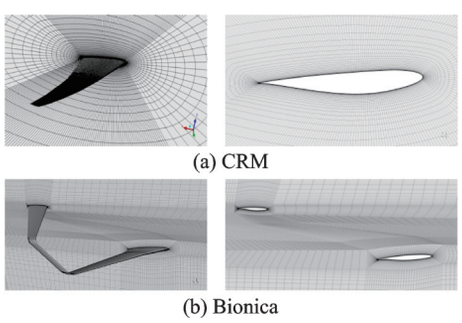
(a) CRM

(b) Bionica

Fig.5 CFD mesh for base configuration of CRM and Bionica wings and their detailed views on the right side

regularity (Eriksson skewness of 0.5—1.0). This mesh density was determined through a prior grid convergence study with the CRM baseline wing, using meshes ranging from 0.5 to 6 million cells. Each planform then undergoes CFD simulation using a commercial software, following the protocol from our previous study[31] that utlises k-ephsilon model along the ehanced wall function generates results with 5% error from the baseline model even with coarser grid size. Here, the process is automated through a pre-scripted workflow, handling simulation settings (boundary conditions, turbulence model, etc.), execution, and post-processing in batch mode. All simulations are performed for cruise conditions: $Ma = 0.85$, $Re = 30\times10^6$, and $\alpha = 2.20^\circ$ for CRM, and $Ma = 0.2$, $Re = 6\times10^6$, and $\alpha = 0^\circ$ for Bionica.

2.4 Constitution of ML models

The proposed optimization framework includes developing a ML prediction model as a central component. This study initially evaluates two models: RF and XGBoost, both effective for small datasets. Previous studies[25-26] have shown XGBoost superior performance over other ML models and traditional CFD approaches in aerodynamic optimization for tube wing and box wing designs. Therefore, XGBoost is selected as the final ML model in this study. The model's performance is assessed by a multi-output regressor from the scikit-learn library, configured with identical datasets. Evaluation occurs in two stages: Through cross-validation during training, and by testing the model on a separate dataset to assess its predictive accuracy.

The models are trained using 80% of the dataset, with prediction capabilities assessed via the mean square error. An objective function in the script iteratively adjusts algorithm parameters to minimize mean absolute error (MAE). Once optimal parameters are achieved, performance is further evaluated using the remaining 20% of the dataset. A tolerance limit of 10% from predicted values is set, acknowledging aerodynamic complexities, as a criterion for surrogate model acceptance. The evaluation shows the XGBoost model achieves an average error of 6%, making it the optimal choice for the next stages of the process.

2.5 Optimization problem definitions

The next step involves integrating the surrogate model with the optimizer and defining the optimization problems. The primary objective is to minimize the aerodynamic drag coefficient (C_D) while satisfying lift coefficient (C_L) constraints. For CRM, the C_L constraint is based on available research data ($C_L = 0.50$)[19]. In contrast, for the Bionica box-wing, where the design is still in early stages, the C_L constraint is not yet finalized. Therefore, the optimization goal for Bionica is to maximize C_L while minimizing C_D.

To address this, a multi-objective optimization model is developed using the NSGA-Ⅱ. This approach is particularly useful for handling diverse objectives, such as minimizing weight and reducing noise across various disciplines. The model is also capable of handling single-objective aerodynamic optimization, as in the case of CRM. To achieve this, the C_L constraint is transformed into an additional minimization objective, aiming to reduce the absolute error between the specified C_L constraint and the ML-predicted C_L (Tables 5,6).

Table 5 CRM Optimization problem definition

Objective	Variable	Constraint
Min. $f(x)=C_D$	ε(5 control points) T/C(3 control points) γ(2 control points) $\Lambda_{c/4}$(1 parameter) $b/2$(1 parameter)	$C_L=0.50$ $Ma=0.85$ $Re=30\times10^6$

Table 6 Bionica optimization problem definition

Objective	Variable	Constraint
Min. $f(x)=C_D$ Max. $f(x)=C_L$	ε(5 control points) T/C(3 control points) γ(3 control points) $\Lambda_{c/4}$(2 parameters) $b/2$(1 parameter)	$Ma=0.2$ $Re=6\times10^6$

3 Results and Discussion

This section presents the results obtained using the proposed methodology, divided into two parts: Validation of the methodology and optimization out-

comes. The CRM and Bionica baseline results are shown to assess the accuracy of the parameterization, computational approach, and machine learning models. The optimization results section showcases the final outcomes of the methodology for both the CRM and Box wing configurations.

3.1 Results validations

As part of the validation, this study adopts the same flight conditions used by Lyu et al.[10], which differ from the operating conditions applied during the optimisation phase. Fig.6 presents CFD results for the baseline CRM wing at flow conditions $Ma = 0.85$, $\alpha = 2.20°$, though at a lower Reynolds number ($Re = 5\times10^6$) and the result is compared against the Lyu et al. study. Although the dataset generation and optimization were conducted using the coarse grid[10], the validation results were obtained with the finest grid resolution of the model, consisting of approximately six million cells. This resolution was achieved by refining the coarse mesh three times in both the streamwise and normal directions relative to the flow. The present results are compared with data in Ref.[10], which were obtained under the same flow conditions but using a different CFD solver. The comparison shows good agreement, both in pressure distribution over the wing's suction side (Fig.6(a)) and pressure coefficient (C_P) along the span (Figs.6(b,c)).

Minor discrepancies may arise from slight differences in twist distribution, as this parameterization is based on a different study[19], and from a lower mesh density used to reduce computational cost for the 160 planform simulations. Nonetheless, the results are acceptable, as demonstrated by the L/D coefficients, $C_L = 0.5$ and $C_D = 0.020\ 8$, which are close to the reference values ($C_L = 0.5$, $C_D = 0.019\ 9$)[10].

The small discrepancies are likely due to the cumulative effect of minor uncertainties in both airfoil and planform parameterization. In particular, the residual differences come from variations in the twist distribution. The present results are compared with study in Ref.[10], which used a different twist, while this study follows the original CRM baseline twist defined in the original study[19]. Furthermore, it is well documented that CRM CFD results show minor variability depending on the mesh type (e.g., hexahedral, polyhedral, or tetrahedral) and the choice of turbulence model[17-19]. Since the purpose of this study is to establish a baseline for subsequent wing optimization, the current results are considered sufficiently accurate and robust for further analysis.

The Bionica CFD simulations are conducted following several grid convergence studies, with the grid converging at 1.7 million cells. The simulation produces results consistent with the previous study of the Bionica geometry[26], showing only a 0.5% difference in C_D (Fig.7). This cross-verification, along with the CRM validation, justifies the reliability of the adopted approach in accurately simulating aerodynamic performance.

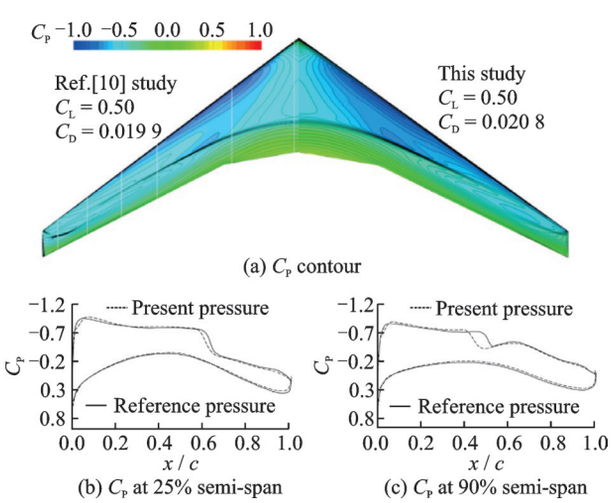

Fig.6 CRM planform within a steady flow (Ma= 0.85, $Re = 5\times10^6$, $\alpha = 2.20°$), as CFD-simulated and compared against results from Ref.[10]

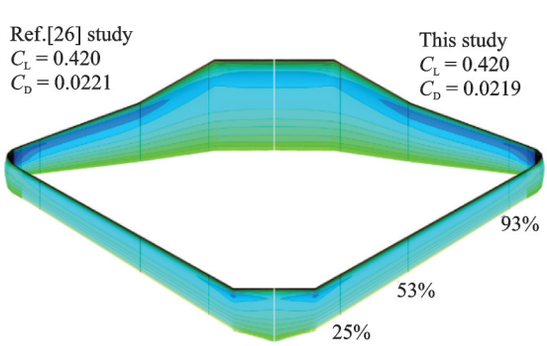

Fig.7 Bionica planform within a steady flow (Ma= 0.2, $Re = 6\times10^6$, $\alpha = 0.0°$), as CFD-simulated and compared against results from Ref.[26]

3.2 Optimization outcomes

The optimized CRM wing planform shows several key improvements over the baseline design. The span has been increased from 58.8 m to 61.5 m (Table 7), suggesting a design shift towards greater aerodynamic efficiency and potential lift enhancement. Additionally, the leading-edge sweep angle has been significantly increased from 37.2° to 43.2°, which likely contributes to improving drag performance at higher speeds by delaying flow separation. In terms of twist distribution, adjustments are made across various spanwise locations. For instance, at 10% and 18% of the span, the twist angles have been increased, enhancing the lift at these sections. Conversely, the negative twist at mid-to-outboard sections ($\eta = 0.37$ to $\eta = 1$) has been reduced, which suggests better control of aerodynamic loads and improved overall efficiency. These changes reflect a refined balance between lift distribution and induced drag. The dihedral angle, represented by the vertical deflection at the tip, shows a slight reduction between 2.36 — 2.33 m, indicating marginal adjustments to wingtip aerodynamics and stability. Finally, the mean thickness-to-chord ratio $(T/C)_m$ has been slightly decreased from 0.113 to 0.109, likely aiming at reducing profile drag without significantly compromising structural integrity. Overall, these optimizations reflect a concerted effort to enhance aerodynamic performance, reduce drag, and improve lift distribution for better cruise efficiency.

The grid convergence study for the CRM optimized planform is illustrated in Fig.8, with drag counts plotted against different grid sizes, ranging from 1.5 million elements to 6.0 million elements. As grid sizes increase, the drag count decreases, demonstrating the impact of mesh resolution. Notably, the largest changes in drag count (Δ) occur between the converged grid sizes of 6 million, where drag counts reduce significantly by 22.97 counts. In terms of aerodynamic performances, this translates into a significant drag reduction (of about 12.3% drag count reduction) of the optimal planform compared to its baseline counterpart.

Table 7 CRM baseline and optimized model comparison

Design parameter	Symbol	Baseline	Optimized
Span	b/m	58.8	61.5
Leading edge sweep	$\Lambda_{L.E.}$/(°)	37.2	43.2
Twist (η =0.10)	$\varepsilon_{10\%}$/(°)	2.15	2.88
Twist (η =0.18)	$\varepsilon_{18\%}$/(°)	0.85	1.78
Twist (η =0.37)	$\varepsilon_{37\%}$/(°)	−0.47	−0.67
Twist (η =0.50)	$\varepsilon_{50\%}$/(°)	−1.72	−1.38
Twist (η =0.70)	$\varepsilon_{70\%}$/(°)	−2.40	−1.62
Twist (η =1)	$\varepsilon_{100\%}$/(°)	−3.75	−3.10
Dihedral (vertical deflection at tip)	z_{tip}/m	2.36	2.33
Mean thickness-to-chord ratio	$(T/C)_m$	0.113	0.109

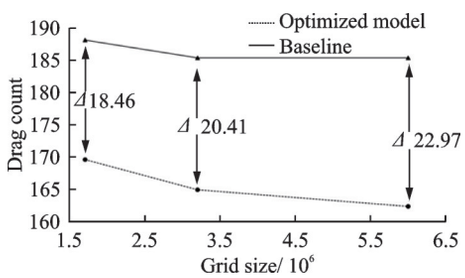

Fig.8 Aerodynamic performances (drag counts = $C_D \times 10\,000$) characterizing the ML-based CRM-based optimal planform and its parameterized baseline counterpart, as estimated using CFD and a grid convergence, simulated for $C_L = 0.5$ at $Re = 30 \times 10^6$

The aerodynamic improvements are attributed to the specific pressure distribution of the optimized planform (Fig.9). Compared to the baseline, the optimized wing shows slightly reduced shocks in the inboard section (top of Fig.9), while the outboard section exhibits stronger shocks on the suction surface. Notably, pressure recovery is extended further aft, potentially delaying stall onset, as seen in the trailing-edge region comparison in Fig.9.

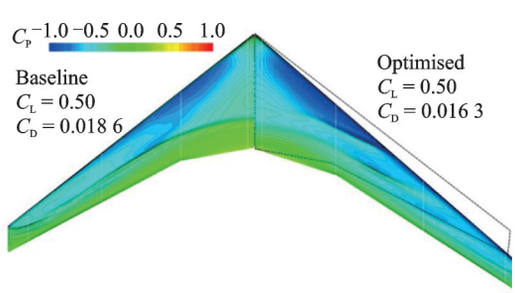

Fig.9 CRM-based optimal planform within a steady flow ($Re = 30 \times 10^6$, $\alpha = 2.00°$, $C_L = 0.5$), as CFD-simulated and compared against its baseline counterpart under similar flow conditions

The comparison between the baseline and optimized Bionica models shows targeted geometric modifications to enhance aerodynamic performance. The front wing's leading-edge sweep has been increased slightly, moving from 18.46° to 19.20° till 20% of the span and decreases in the outboard section from 23.46° to 21°, improving high-speed lift characteristics (Table 8). Twist angles (ε) have been introduced at various span locations in the optimized design, which likely improves aerodynamic efficiency and load distribution. Dihedral angles (γ) have been slightly increased for the front wing, contributing to better lateral stability, while thickness-to-chord ratios (T/C) have been reduced, particularly at the wingtip, to minimize drag.

Table 8 Bionica baseline and optimized model comparison

Wing	Parameter	Baseline	Optimized
Front wing	$\Lambda_{0.2(c/4)}$/(°)	18.46	19.22
	$\Lambda_{1.0(c/4)}$/(°)	23.46	21.0
	$\varepsilon_{0.0}$/(°)	0.0	5.0
	$\varepsilon_{0.4}$/(°)	0.0	3.6
	$\varepsilon_{1.0}$/(°)	0.0	1.5
	$\gamma_{0.4}$/(°)	15.0	16.0
	$\gamma_{1.0}$/(°)	17.0	16.60
	$T/C_{0.0}$	0.11	0.084
	$T/C_{0.4}$	0.11	0.07
	$T/C_{1.0}$	0.11	0.05
Rear wing	$\Lambda_{1.0(c/4)}$/(°)	−20.56	−22.60
	$\varepsilon_{0.0}$/(°)	0.0	2.8
	$\varepsilon_{1.0}$/(°)	0.0	−0.9
	$\gamma_{1.0}$/(°)	0.0	−1.00
	$T/C_{0.0}$	0.11	0.09
	$T/C_{1.0}$	0.11	0.09
Winglet	Λ_w/(°)	30.0	29.20

In the rear wing, the leading-edge sweep is marginally adjusted, moving from −20.56° to −22.60°, potentially enhancing stability. Twist angles are also introduced here, with root twist increasing to 2.8° and tip twist slightly negative at −0.9°, which may help manage load distribution between the wings. The rear wing thickness-to-chord ratio (T/C) has also been reduced slightly, likely contributing to reduced drag. The winglet's sweep remains relatively consistent, with only a slight decrease from 30° to 29.20°, balancing control of wingtip vortices. These adjustments reflect a comprehensive optimization effort aiming at improving aerodynamic efficiency and stability.

Once the ML based surrogate model provides the optimized planform for the Bionica wing, a grid convergence study of the configuration is performed. The grid convergence study in Fig.10 applies different grid resolutions to assess the accuracy of the Bionica optimized model. As the grid size increases, the results stabilize, indicating that a grid size of around 6 million cells is sufficient to capture the aerodynamic performance accurately. For the converged results, C_L is 0.58, while C_D is 0.026. This yields a L/D ratio, that is, C_L/C_D of approximately 22.3, indicating a significant improvement (about 18%) of overall aerodynamic performance. It demonstrates the proposed optimization process can effectively optimize both tube wing (CRM) and Bionica (box wing).

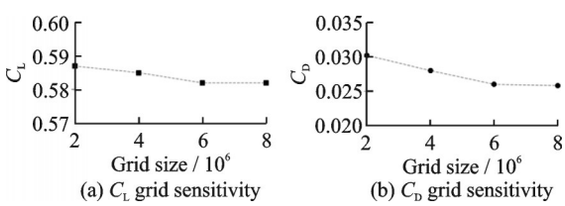

Fig.10 Aerodynamic performances characterizing the ML-based Bionica optimal planform C_D and C_L, as estimated using CFD and a grid convergence, simulated at $Re = 6\times10^6$

The C_P plots in Figs.11,12 show significant improvements in the optimized Bionica wing compared to the baseline. Across all span-wise sections, the optimized wing (dashed lines) exhibits a stronger suction peak near the leading edge, indicating enhanced lift generation. Additionally, the optimized wing shows a smoother pressure recovery from mid-chord to the trailing edge, which is particularly important in reducing flow separation and drag.

In the outboard sections, the optimized wing maintains a slightly higher negative C_P value at the leading edge, suggesting a more favorable pressure gradient and improved aerodynamic performance. These modifications contribute to better overall lift

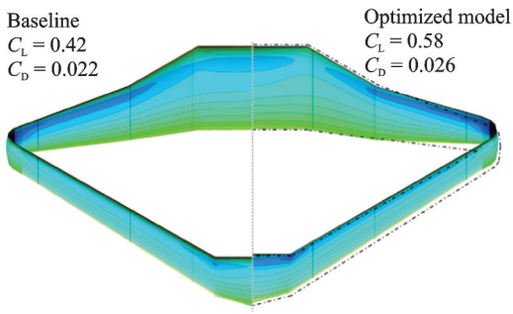

Fig.11 Static pressure distribution over the suction side of baseline and optimal Bionica planform for the finer grid, simulated at $Re = 6\times10^6$

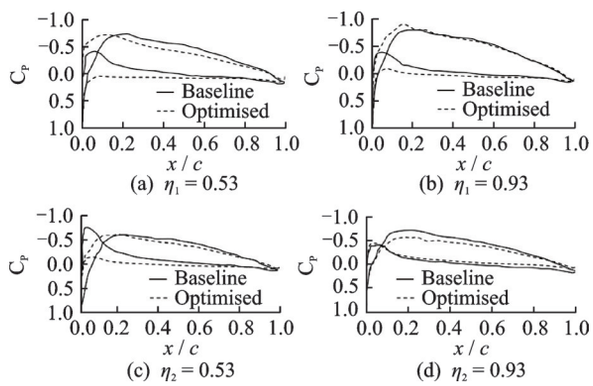

Fig.12 Comparison of C_P distribution between baseline and optimized Bionica wing across various spanwise sections presented in the fraction of the span and η_1 for front wing while η_2 for rear wing

distribution while minimizing drag. The optimized pressure distribution is a clear indicator of the improvements in aerodynamic efficiency, with enhanced lift characteristics and a reduction in drag, making the optimized design more effective for performance at cruise conditions.

4 Conclusions

This study presents a ML-based methodology for optimizing the aerodynamic performance of both conventional (CRM) and non-conventional (Bionica box-wing) aircraft configurations. By employing advanced parameterization techniques, such as CST and Bezier curves, the method effectively reduces the number of design variables while maintaining design flexibility. Multiple planforms are generated within the defined design space, followed by validated CFD simulations, which are used to build a comprehensive CFD database for training the machine learning model.

The XGBoost model was selected for its superior predictive accuracy in this context. The optimization process, executed through the NSGA-Ⅱ, leads to significant aerodynamic gains. For the CRM wing, a 12.3% reduction in drag is achieved compared to the baseline, while the Bionica box-wing configuration sees an 18% improvement in the L/D ratio (C_L/C_D). These results demonstrate the effectiveness of combining ML with traditional optimization techniques, offering a computationally efficient approach to improve aerodynamic performance in both conventional and unconventional aircraft designs.

References

[1] BREZILLON J, DWIGHT R. Aerodynamic shape optimization using the discrete adjoint of the navier-stokes equations: Applications towards complex 3D configurations[C]//Proceedings of the CEAS/KATNet Ⅱ Conference on Key Aerodynamic Technologies. Bremen, Germany: machtWissen. de AG, 2009: 1-8.

[2] FREDIANI A, CIPOLLA V, RIZZO E. The PrandtlPlane configuration: Overview on possible applications to civil aviation[M]//Variational Analysis and Aerospace Engineering: Mathematical Challenges for Aerospace Design. Boston, USA: Springer, 2012: 179-210.

[3] MASTERS D A, POOLE D J, TAYLOR N J, et al. Impact of shape parameterisation on aerodynamic optimisation of benchmark problem[C]//Proceedings of the 54th AIAA Aerospace Sciences Meeting. San Diego, USA: AIAA, 2016: 1544.

[4] CARRIER G, DESTARAC D, DUMONT A, et al. Gradient-based aerodynamic optimization with the elsA software[C]//Proceedings of the 52nd Aerospace Sciences Meeting. National Harbor, USA: AIAA, 2014: 0568.

[5] WU E, MADER C A, MARTINS J R R A. A gradient-based sequential multifidelity approach to multidisciplinary design optimization[J]. Structural and Multidisciplinary Optimization, 2022, 65(4): 131.

[6] ADLER E J, MARTINS J R R A. Efficient aerostructural wing optimization considering mission analysis[J]. Journal of Aircraft, 2023, 60(3): 800-816.

[7] DAM B, PIRASACI T, KAYA M. Artificial neural network based wing planform aerodynamic optimiza-

tion[J]. Aircraft Engineering and Aerospace Technology, 2022, 94(10): 1731-1747.

[8] BROOKS T R, KENWAY G K, MARTINS J R R A. Undeflected common research model (uCRM): An aerostructural model for the study of high aspect ratio transport aircraft wings[C]//Proceedings of the 35th AIAA Applied Aerodynamics Conference. Denver, USA: AIAA, 2017: 4456.

[9] PATRI A, PATNAIK Y. Random forest and stochastic gradient tree boosting based approach for the prediction of airfoil self-noise[J]. Procedia Computer Science, 2015, 46: 109-121.

[10] LYU Z J, KENWAY G K, MARTINS J R R A. RANS-based aerodynamic shape optimization investigations of the common research model wing[C]//Proceedings of the 52nd Aerospace Sciences Meeting. National Harbor, USA: AIAA, 2014: 0567.

[11] CHEN S, LYU Z J, KENWAY G K W, et al. Aerodynamic shape optimization of common research model wing-body-tail configuration[J]. Journal of Aircraft, 2016, 53(1): 276-293.

[12] HALILA G L O, MARTINS J R R A, FIDKOWSKI K J. Adjoint-based aerodynamic shape optimization including transition to turbulence effects[J]. Aerospace Science and Technology, 2020, 107: 106243.

[13] KOCHKOV D, SMITH J A, ALIEVA A, et al. Machine learning-accelerated computational fluid dynamics[J]. Proceedings of the National Academy of Sciences of the United States of America, 2021, 118(21): e2101784118.

[14] TAGHIZADEH S, WITHERDEN F D, HASSAN Y A, et al. Turbulence closure modeling with data-driven techniques: Investigation of generalizable deep neural networks[J]. Physics of Fluids, 2021, 33(11): 115132.

[15] WASCHKOWSKI F, ZHAO Y M, SANDBERG R, et al. Multi-objective CFD-driven development of coupled turbulence closure models[J]. Journal of Computational Physics, 2022, 452: 110922.

[16] ZHANG X S, XIE F F, JI T W, et al. Multi-fidelity deep neural network surrogate model for aerodynamic shape optimization[J]. Computer Methods in Applied Mechanics and Engineering, 2021, 373: 113485.

[17] TAO J, SUN G. Application of deep learning based multi-fidelity surrogate model to robust aerodynamic design optimization[J]. Aerospace Science and Technology, 2019, 92: 722-737.

[18] ZHANG Z Q, LI P J, LI Q K, et al. Dynamic machine learning global optimization algorithm and its application to aerodynamics[J]. Journal of Propulsion and Power, 2023, 39(4): 524-539.

[19] VASSBERG J, DEHAAN M, RIVERS M, et al. Development of a common research model for applied CFD validation studies[C]//Proceedings of the 26th AIAA Applied Aerodynamics Conference. Honolulu, USA: AIAA, 2008: 6919.

[20] FONSECA L, FONSECA L M. From quality gurus and TQM to ISO 9001: 2015: A review of several quality paths[J]. International Journal for Quality Research, 2016, 9(1): 167-180.

[21] HOYLE D. ISO 9000 quality systems handbook[M]. London, UK: Butterworth-Heinemann, 2001.

[22] ISO. The process approach in ISO 9001: 2015[EB/OL]. [2023-09-11]. http://www.iso.org.

[23] CIAMPA P, ZILL T, NAGEL B. CST parametrization for unconventional aircraft design optimization[C]//Proceedings of the 27th International Congress of the Aeronautical Sciences. [S.l]: ICAS, 2010.

[24] KULFAN B M. Universal parametric geometry representation method[J]. Journal of Aircraft, 2008, 45(1): 142-158.

[25] HASAN M, KHANDOKER A, GESSL G, et al. Low fidelity data driven machine learning based optimisation method for box-wing configuration[J]. Aerospace Science and Technology, 2024, 150: 109169.

[26] HASAN M, AZAD K. Enhancing box-wing design efficiency through machine learning based optimization[J]. Chinese Journal of Aeronautics, 2025, 38(2): 103216.

[27] HELMREICH J E. Regression modeling strategies with applications to linear models, logistic and ordinal regression, and survival analysis[M]. Cham, Switzerland: Springer, 2015.

[28] AUSTIN P C, STEYERBERG E W. The number of subjects per variable required in linear regression analyses[J]. Journal of Clinical Epidemiology, 2015, 68(6): 627-636.

[29] ZOU M, JIANG W G, QIN Q H, et al. Optimized XGBoost model with small dataset for predicting relative density of Ti-6Al-4V parts manufactured by selective laser melting[J]. Materials, 2022, 15(15): 5298.

[30] MAHMOOD R, LUCAS J, ACUNA D, et al. How much more data do i need? Estimating requirements for downstream tasks[EB/OL]. (2022-07-04). https://doi.org/10.48550/arXiv.2207.01725.

[31] HASAN M, REDONNET S, HERNADI A. Computational investigation of a novel box-wing aircraft concept[J]. Applied Sciences, 2022, 12(2): 752.

Acknowledgement We would like to extend our sincere gratitude to Azad Khandoker from JKU Linz for his continuous support and guidance in research and innovation, which served as a major inspiration for this study. Our heartfelt thanks also go to the Bionica-aircraft team for their valuable resources, insightful feedback, and constructive criticism, which significantly improved the quality of this manuscript.

Authors

The first author Mr. **HASAN Mehedi** is a postdoctoral researcher at Hangzhou International Innovation Institute, Beihang University. His current research focuses on sonic boom minimization using artificial intelligence. He received his Ph. D. from Beihang University in 2025, where he developed an AI-based multidisciplinary aerodynamic optimization framework. His research experience includes UAV design and box-wing configurations. His expertise covers computational fluid dynamics, aerostructural optimization, machine learning, and finite element analysis.

The corresponding authors Prof. **DENG Zhongmin** is a professor at School of Astronautics, Beihang University. His current research focuses on composite structural analysis and design, flight vehicle structural dynamics and control, and spacecraft dynamics and control. He has extensive experience in high-level numerical modeling and structural mechanics applied to aerospace systems. He has led and participated in multiple national research projects and has published widely in peer-reviewed international journals and conferences. Mr. **REDONNET Stéphane** is an assistant professor in mechanical and aerospace engineering at Hong Kong University of Science and Technology. Prior to his current appointment, he served as a senior researcher at ONERA and collaborated extensively with NASA as a visiting researcher. His research focuses on numerical simulation, computational aeroacoustics, unsteady flow modelling, and aerodynamic noise prediction.

Author contributions Mr. **HASAN Mehedi** developed the concept, designed the methodology, performed validation and optimization, and wrote the manuscript. Prof. **DENG Zhongmin** contributed to concept development, supervised the methodological framework, assisted in drafting the manuscript, and provided resource allocation. Mr. **REDONNET Stéphane** contributed to concept development, co-drafted the manuscript, and supervised the optimization section. Mr. **SANUSI B. Muhammad** proofread the manuscript and contributed to visualization. All authors commented on the manuscript draft and approved the submission.

Competing interests The authors declare no competing interests.

(Production Editor: ZHANG Bei)

翼型盒式机翼布局的气动优化及其机器学习集成方法

哈桑·梅赫迪[1], 邓中敏[1], 雷东内·斯特凡[2], 萨努西·B.穆罕默德[3]

(1.北京航空航天大学杭州创新研究院,杭州 310020,中国; 2.香港科技大学机械与航空航天工程系,香港 999077, 中国; 3.哈尔滨工业大学(深圳) 机电工程与自动化学院,深圳 518057,中国)

摘要:本文提出了一种基于机器学习的机翼气动性能优化方法,适用于常规布局(Common research model, CRM)机翼和非传统布局,即Bionica盒式机翼。该方法通过采用先进的参数化技术如类别/形状变换(Class and shape transformation, CST)函数与Bezier曲线在降低设计复杂性的同时保持了几何建模的灵活性。利用计算流体力学(Computational fluid dynamics, CFD)仿真生成的综合数据集训练了extreme gradient boosting (XGBoost)模型,以预测气动性能。在此基础上,采用非支配排序遗传算法进行优化。结果表明,CRM机翼的阻力降低了12.3%,而Bionica盒式机翼的升阻比提高了18%。研究结果验证了基于机器学习的优化方法在气动设计中的有效性,并显著提升了在不同构型下的效率。

关键词:气动优化;盒式机翼;机器学习;计算流体力学